

The object of this study is a high-speed railroad vehicle. The introduction of high-speed traffic on Ukrzaliznytsia is constrained by the structure of the track, which has up to 30% of curved sections where the speed is limited in terms of traffic safety and passenger comfort. In addition, with increasing speed, the wear of wheel rims increases significantly. This gives rise to the problem of organizing high-speed traffic. One direction to solve it (very expensive) is to design a high-speed track where curved sections are absent or have a radius of several kilometers. Another option (less expensive) is to design vehicles with devices that partially compensate for centrifugal force – gravitational, by tilting the body. To reduce the wear of wheel rims, systems for radial installation of wheelsets in curves are quite effective.

Almost 50 years of experience in using radial wheelset and body tilt systems on curved track sections in Switzerland, Norway, etc. proves their high efficiency in solving the problems of rim wear and passenger comfort.

The study reported here was conducted by computer simulation. For this purpose, a mathematical model of the dynamics of high-speed rail vehicle movement along a curved track section with a radius of 350 m and an increase in the outer rail by 0.15 m was synthesized. The feasibility of simultaneously equipping vehicles with systems for forced radial wheelsets and forced body tilt has been proven.

On routes containing 30% of curves with a radius close to 350 m, this will reduce train travel time by 8.3%. This percentage will increase proportionally in accordance with the increase in the length of curved sections along the route

Keywords: railroad transport, radial installation, wheelset, body inclination, undamped acceleration

UDC 625.032.07

DOI: 10.15587/1729-4061.2025.330924

DETERMINATION OF THE EFFECTIVENESS OF THE APPLICATION OF RADIAL WHEEL PAIR INSTALLATION AND BODY TILT ON HIGH-SPEED VEHICLES WHEN DRIVING ON CURVED SECTIONS OF THE TRACK

Vyacheslav Masliev

Corresponding author

Doctor of Technical Sciences, Professor*

E-mail: masliev@ukr.net

Oleksandr Yakunin

PhD Student*

*Department of Electric Transport and Diesel Locomotive Engineering

National Technical University «Kharkiv Polytechnic Institute» Kyrpychova str., 2, Kharkiv, Ukraine, 61002

Received 03.03.2025

Received in revised form 14.04.2025

Accepted 20.05.2025

Published 27.06.2025

How to Cite: Masliyev, V., Yakunin, O. (2025). Determination of the effectiveness of the application of radial wheel pair installation and body tilt on high-speed vehicles when driving on curved sections of the track. *Eastern-European Journal of Enterprise Technologies*, 3 (7 (135)), 40–49. <https://doi.org/10.15587/1729-4061.2025.330924>

1. Introduction

The prospect of Ukraine's accession to the European Union necessitates a deep modernization of Ukrzaliznytsia (UZ) – its track and transport. First of all, this concerns its passenger component, where the speeds are significantly lower than in Europe. The reasons relate to the design of the track, which is not adapted to high-speed traffic, in particular because of the fact that it has about 30% of curved sections where the speed is limited by a number of conditions. They are related to the need to ensure the safety of traffic in the event of derailment of wheels, and passenger comfort – at an acceptable level ($0.7\text{--}0.8\text{ m/s}^2$) of “undamped acceleration” transverse to the direction of the track. In addition, with increasing speed, the wear of wheel rims increases approximately according to quadratic law.

Therefore, a problem arises regarding the implementation of high-speed traffic on Ukrzaliznytsia. There are two known solutions. The first of them, which is too expensive, involves building a high-speed track network where there are no curved sections or having large (several kilometers) radii of curvature. A second way, which is much less expensive, involves equipping high-speed rolling stock with special sys-

tems. One of them is a system for tilting the body to the center of the curved section of the track in order to compensate for the centrifugal component of the “undamped acceleration” using gravitational force. Such systems (mechanical, hydraulic, electromechanical – by design and principle of operation) are widely used internationally and have achieved a certain technical and operational perfection. Meanwhile, each of them has its disadvantages, which are due to the complexity of the structure, its excessive weight and dimensions, as well as energy consumption.

Full-scale dynamic and track studies of vehicles (Vs), which are mandatory for new Vs, are very time-consuming and costly, due to the fact that they require their conduct under all possible operating conditions.

It is possible to reduce costs somewhat by conducting Vs studies at the design stage through mathematical modeling.

Meanwhile, during mathematical modeling, numerous assumptions are introduced, as a result of which important information regarding the influence of individual factors on the results may be lost. This is often due to the desire of researchers to reduce the volume of calculations and computer time.

For example, when modeling the dynamics of vehicle movement on curved sections of the track, researchers often

introduce the angles of contact of the wheel rims on the rails into the equations – as constants. In fact, these angles are functions of many parameters of the wheel-rail system and V_s movement conditions. As a result, errors arise when calculating the wear indicators of wheel rims and traffic safety.

In this regard, scientific research aimed at synthesizing adequate mathematical models of vehicle motion dynamics, which take into account in detail the features of the “rolling stock – track” system, continues to remain a relevant task.

2. Literature review and problem statement

In work [1], it is shown that high-speed transport (HST) is recognized as promising in all countries of the world due to its high carrying capacity, safety, and comfort for passengers, reduction of travel time, independence from weather conditions, etc. Therefore, its development should be a priority of state policy in the transportation industry. The financial and economic sustainability of investments in HST was also analyzed. The conclusion is that a developing country can set affordable prices for high-speed rail services and at the same time achieve financial viability, but this requires a very high passenger density. But the issues related to the problems of HST operation are not covered. Perhaps this is not disclosed in order not to discriminate against the very idea of HST.

In work [2], it is noted that only a few studies have focused on the actual operational characteristics of HST, which is becoming one of the most important modes of transport in the world. Compared with airplanes and other types of land transport, it has such characteristics as comfort, safety, high capacity, and high speed. Since HST is an expensive project, operational efficiency is important for its sustainable development, and insufficient demand for passenger transportation can lead to significant losses. However, issues related to the organization of operation on HST lines together with freight rolling stock remain unresolved.

In [3], ways of developing high-speed passenger traffic on UZ are proposed. The concepts of organizing high-speed traffic in the world are analyzed. This is the concept of a separate high-speed traffic system following the example of Japan and Spain and the concept of combined use of tracks for high-speed and freight traffic following the example of Germany, Italy, and Poland. The advantages and disadvantages of each of the concepts are analyzed. The patterns of degradation processes in the rail track during operation on high-speed lines together with freight traffic are determined. Some requirements for the design of the track intended for high-speed passenger traffic combined with freight traffic are determined. Meanwhile, the authors do not pay enough attention to the problem of the influence of increasing speed on such relevant indicators as the wear of wheel rims and passenger comfort when moving along curved sections of the track. Perhaps these problems require separate research. But they cannot be ignored when organizing high-speed traffic on a regular track, where there are many curved sections.

In work [4], the process of force interaction between the railroad track and rolling stock under conditions of accelerated movement on a straight section was experimentally investigated. The average values of stresses were established: in the rails they are 44.37...70.99 MPa; in the sleeper 0.78 MPa; in the ballast layer 0.13 MPa; in the subgrade 0.04 MPa, which is significantly less than the maximum permissible values. With an increase in the speed of movement from

140 to 176 km/h, the values of the parameters decrease within 8–20%. Thus, it was established that with the existing structure of the railroad track on straight sections, it is possible to increase the speed of movement of vehicles. But the issues related to increasing the speed of movement along curved sections remained unresolved.

In [5], the results of simulation tests of a subway car are reported, which were conducted on a track with a radius of a curve of 300 m, where the wear of wheels and rails is the greatest. This is especially observed in the case of high stiffness of the connections of the wheelsets with the bogie frame. The authors see the solution to the wear problem in the use of radial installation of wheelsets in curves. It is implemented by using connections of the wheelsets with the bogie frame with variable stiffness in the horizontal plane. The study has shown that the wear of wheels on the curved section of the track is significantly reduced. However, the possibility of increasing the speed of movement on curved sections remain unresolved.

In [6], it is stated that proper comfort for passengers can be ensured by equipping vehicles with systems that operate on the principle of compensation for unsettled acceleration. Meanwhile, mechanical, hydraulic, and electromechanical systems have inherent disadvantages due to the complexity of the design and weight-dimensional indicators. The combined system of tilting the body of a high-speed vehicle was studied by modeling. The dependences of the electrical and pneumatic indicators of the system over time, namely converters, air springs, etc., were determined. However, the system has become significantly more complicated compared to known ones, and for its production, operation, and repair it is necessary to train many high-level specialists, which requires a certain amount of time and costs.

In work [7], the impact of foreign technology transfer on domestic innovations in the context of the implementation of high-speed railroads in China was assessed. Technological similarity, rather than the “input-output” relationship, plays a dominant role in explaining the importance of knowledge flow both at the firm level and at the aggregate level. The conclusion is drawn about the importance of absorptive capacity in the assimilation of foreign technologies for the accelerated construction of high-speed railroads. However, questions remain regarding overcoming certain obstacles in this process, which are caused by competition in the market.

The perfect (with a minimum of defects) system was studied in [6], in which it was proposed to tilt the vehicle body around its longitudinal axis at a set angle using an electromechanical servo device. The operation of the system was studied, and its effectiveness was proven. However, the authors did not pay enough attention to the study of oscillatory processes that would arise under the action of lateral excitations from the rails.

In [8], the high efficiency of conducting research using a methodology that involves the use of methods of mathematical modeling of complex mechanical systems together with computer technologies was proven. But not enough attention was paid to checking the adequacy of the mathematical modeling of the technical system that was studied.

In [9], a mathematical model of locomotive dynamics during high-speed movement is described. The model takes into account nonlinear elastic and dissipative characteristics of its constituent elements and makes it possible to predict dynamic and operational indicators at the design stage of the locomotive. The adequacy of the model was verified by

comparing the theoretical and experimental results of tests of diesel locomotives of the TE109 and 2TE116 series. The dependences of the relative magnitudes of the steering forces on the stiffness of the axle box connections with the bogie frame were obtained. It was proven that the stiffness of the connections significantly affects the level of steering forces on the track, which has horizontal irregularities on the rails. However, when compiling the model, the authors did not pay enough attention to the detailed consideration of the train movement modes with this locomotive.

In [10], the problems of the dynamics of the movement of diesel locomotives equipped with devices that reduce the wear of the ridges and rolling surfaces of the wheel bands are considered. Mathematical models of diesel locomotives are compiled taking into account the operation of these devices when moving along curved sections of the track. The factors on which wear depends are ranked in importance. A method for predicting the wear of rims of the wheel bands is proposed. However, when compiling the model, the author of the work did not pay enough attention to the possible significant increase in vehicle speeds in the future.

All this gives grounds to assume that it is advisable to conduct a study aimed at identifying the consequences of increasing vehicle speeds and applying systems for radial installation of wheelsets and body tilt on them.

3. The aim and objectives of the study

The purpose of our study is to identify the consequences of increasing the speed of vehicles on the Ukrzaliznytsia track and applying systems for radial installation of wheelsets and body tilt on them. This will provide an opportunity to accelerate the solution to the problem of introducing high-speed traffic on the existing Ukrzaliznytsia track.

To achieve the goal, the following tasks were set:

- to synthesize a mathematical model of the movement of a high-speed railroad vehicle equipped with systems for radial installation of wheelsets and body tilt;
- to investigate the effectiveness of the use of systems that will ensure passenger comfort and the wear of vehicle wheel rims within the established limits.

4. The study materials and methods

The object of our study is a high-speed railroad vehicle equipped with systems for radial installation of wheelsets and body inclination, moving along curved sections of the track. The study was conducted using an example of Ukrainian railroads.

The main hypothesis of the study is as follows: it is known that an increase in the speed of the vehicle significantly increases the wear of wheel rims. In addition, passenger comfort deteriorates due to the increase in the curved sections of the track of the undamped acceleration transverse to its direction. Therefore, taking into account international experience, it can be expected that equipping the vehicle with systems for radial installation of wheelsets and body inclination would make it possible, with increasing speed, to keep the wear of wheel rims and undamped acceleration within the established limits.

It is assumed that the movement of the vehicle along the track, which has curved sections of different curvature with

corresponding elevations of the outer rail, is constant. The track is represented as two elastic beams with irregularities located on a transversely elastic-viscous base. Before the rim starts to touch the side face of the rail, there is no pressing of the rim. The elastic pressing of the rail is calculated as the difference between the modules of the coordinate of the point of contact of the rim with the rail in dynamics and the sum consisting of the “arrow” of the curve arc, the gap in the track and the roughness of the rail in plan. The forces at the contacts of the wheels with the rails are calculated according to the creep theory – on the ascending part of the characteristic, and according to the hypothesis of dry friction – on its descending part. The damping coefficients of the elastic connections are assumed to be constant in all sections of their characteristics. The slopes of the rolling surfaces of all wheels are the same.

The following simplifications are adopted. Longitudinal, vertical vibrations and galloping of the body, bogie frames and wheelsets, as well as lateral vibrations of wheelsets, are neglected. The undercarriage components are considered to be absolutely rigid bodies, the masses of which are concentrated in their “centers of mass” and are interconnected by linear or nonlinear elastic-damping connections.

To reproduce movement along straight sections, it is assumed that the radius of curvature of the track is not less than 10 km. Before the rim of the side face of the rail touches, there is no compression of the rail.

The study was carried out by theoretical methods, by studying the synthesized mathematical model of the dynamics of vehicle movement along the track using the MATLAB software package (USA). The model was checked for adequacy by comparing the calculated elastic compression of the rails with those obtained in the process of dynamic and track tests of a full-scale vehicle, which has a similar undercarriage structure.

The work was performed using the Lagrange algorithm of the second kind and computer technologies, since this is the least time-consuming and costly methodology for synthesizing and researching mathematical models of complex technical systems [8].

5. Research results: synthesis, testing of the mathematical model; determining the dependence of wheel rim wear on the speed of the vehicle

5.1. Synthesis and testing of the mathematical model of the vehicle

A calculation scheme of the vehicle undercarriage was synthesized: Fig. 1, 2. The undercarriage consists of body 1, which is supported through elastically-damping supports 2 on bogies 3, each of which has frame 4 with traction electric motors 5.

Frame 4 is supported by an elastic-damping suspension 6 on axle boxes 7, which are placed on wheelsets 8, which rest on rails 9, which have an elastic-damping connection 10 with the track base. Pivot assembly 11 enables the following connections of frame 4 with body 1: rigid – in the longitudinal direction, rotation – around the vertical axis, and lateral displacements – during deformations of elastic connections 12. Sliders 13 and stops 14 implement the pre-tensioning of elastic connections 12.

In the center of mass of the vehicle body is the origin O_A of the “track” rectangular coordinate system. When the vehicle moves, it also moves along the geometric axis of the track with a constant speed and without any oscillations. The origin O of its “own” rectangular coordinate system is also fixed to the center of mass of the body.

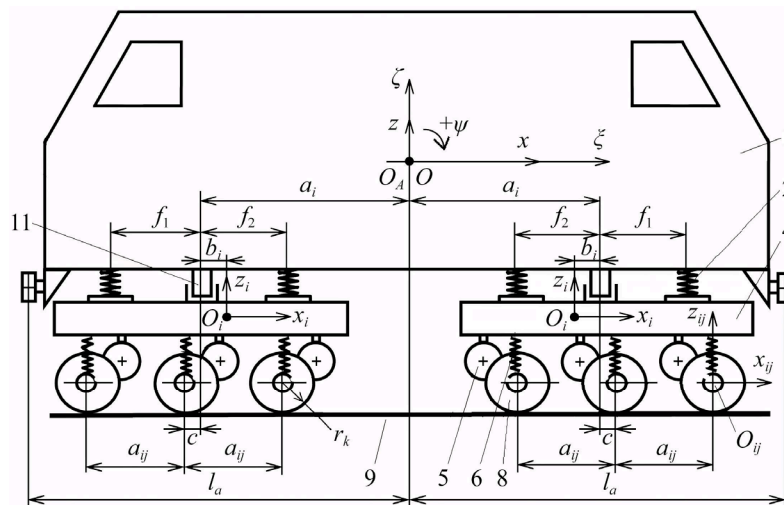


Fig. 1. Undercarriage design diagram, side view: 1 – body; 2 – elastic-damping support; 4 – bogie frame; 5 – traction electric motor; 6 – elastic-damping suspension; 8 – wheelset; 9 – rails; 11 – pivot assembly

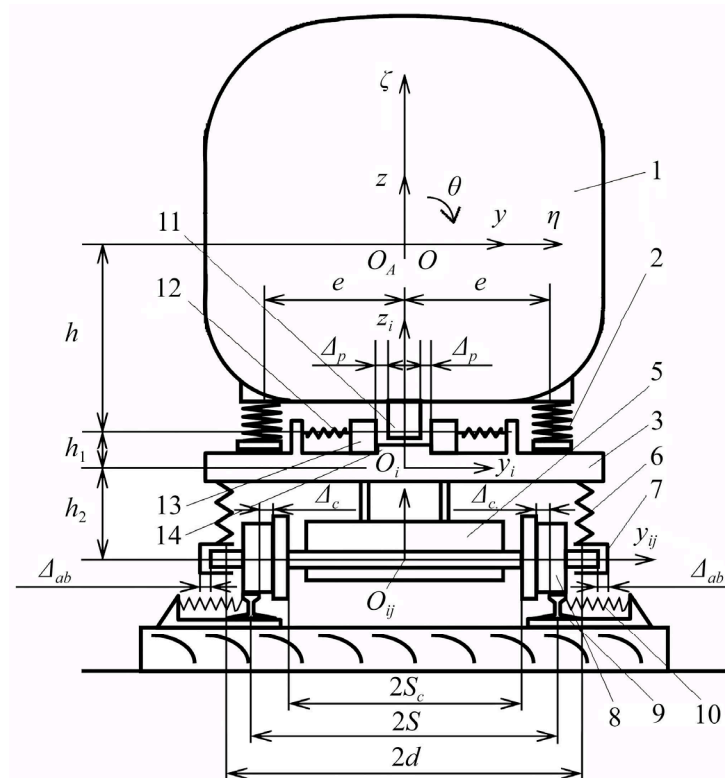


Fig. 2. Undercarriage design diagram, rear view: 1 – body; 2 – elastic-damping support; 3 – bogie; 5 – traction electric motor; 6 – elastic-damping suspension; 7 – axle boxes; 8 – wheelset; 9 – rails; 10 – elastic connection of rails with the track base; 11 – pivot assembly; 12 – elastic connection of the body with the bogie frame; 13 – slider; 14 – stop

The origins of rectangular coordinate systems are fixed to the centers of mass of the bogie frames and wheelsets, O_i and O_{ij} , respectively. Index i determines the bogie frame number, index j determines the number of a wheelset in the bogie. In the center of the curved section of the track, the origin of the fixed rectangular coordinate system O_K is placed (Fig. 3). When the vehicle moves, its mass together with its natural coordinate systems perform small translational movements

and small angular rotations relative to the track coordinate system, and one relative to another. Translational movements of its natural coordinate systems relative to the track coordinate system are determined by the generalized coordinates of the centers of mass of the body ξ, η, ζ , bogie frames ξ_i, η_i, ζ_i , wheelsets $\xi_{ij}, \eta_{ij}, \zeta_{ij}$.

Small translational movements of own coordinate systems relative to each other are determined by the generalized coordinates: $x_i, y_i, z_i, x_{ij}, y_{ij}, z_{ij}$. Angular rotations of the own coordinate systems relative to the longitudinal, transverse, and vertical coordinate axes are determined by the generalized coordinates: body θ, ψ, φ , bogie frames $\theta_i, \psi_i, \varphi_i$, and wheelsets $\theta_{ij}, \psi_{ij}, \varphi_{ij}$.

Table 1 gives the accepted designations of system parameters.

Due to the complexity of V , a mathematical model in the form of differential equations of oscillations was synthesized using the Lagrange algorithm of the second kind

$$\frac{d}{dt} \frac{\partial T_K}{\partial \dot{q}_i} - \frac{\partial T_K}{\partial q_i} + \frac{\partial \Phi}{\partial \dot{q}_i} + \frac{\partial \Pi}{\partial q_i} = Q_i, \quad (1)$$

where T_K , Π and Φ are the kinetic, potential energy, and dissipation function of the system, respectively; Q_i are the components of the generalized force vectors; q_i, \dot{q}_i are the components of the generalized coordinate vectors and generalized velocities of the centers of mass of the system components; $i = 1 \dots n$ is the number of generalized coordinates (degrees of freedom) of the system [10].

The kinetic energy of the system depends on the rates of change of the generalized coordinates; therefore, it is determined using the Koenig theorem

$$T_K = \frac{1}{2} \sum_{i=1}^n A_i \cdot \dot{q}_i^2, \quad (2)$$

where A_i are the inertial coefficients of the system (masses and moments of inertia), \dot{q} are the generalized velocities (linear and angular) of the masses of the system; n is the number of generalized coordinates of the system.

The potential energy of linear elastic bonds between the masses of the system during their deformations according to the Clapeyron theorem

$$\Pi_1 = \frac{1}{2} K_n \cdot q_i^2, \quad (3)$$

where K_n is the stiffness coefficient n of the elastic connection of the system.

The potential energy accumulated in the system due to the lifting of its masses

$$\Pi_2 = \sum_i^n m_i g q_{iz}, \quad (4)$$

where q_{iz} is the projection onto the vertical axis of the change in the generalized coordinate of the center of mass of the component element of the system; g is the acceleration of gravitational forces.

If hydraulic vibration dampers are located parallel to the elastic connections, then the vibration energy dissipation function is

$$\Phi = \frac{1}{2} \sum_i^n \beta_i \cdot \dot{q}_i^2, \quad (5)$$

where β_i are the coefficients of viscous resistance of the vibration damper, the inelastic resistance force of which is proportional to the speed of its rod.

The "generalized" forces Q_i include external forces acting on the contacts of the wheels with the rails, traction (braking) forces, aerodynamic forces, and excitations coming from the track.

Since the generalized coordinates of the system are, by definition, independent of each other, when one of them varies, the others do not vary.

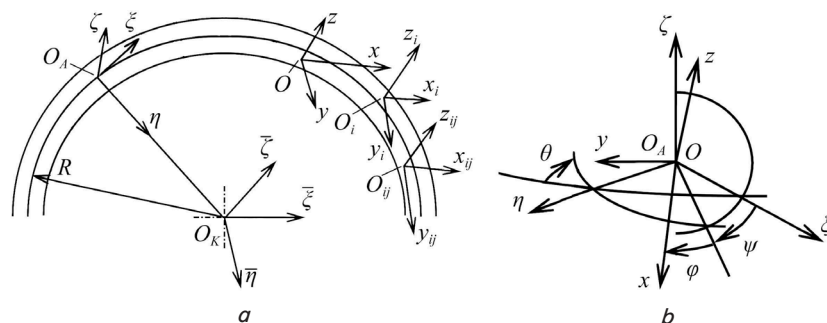


Fig. 3. Coordinate systems: *a* – linear; *b* – angular

Table 1

Accepted system parameter designations

«Base»	Vehicle	$x_{oi} = a_i$
	Bogie	$x_{oij} = a_{ij}$
Coordinates of arbitrary points	Body	x_k, y_k, z_k
	Bogie	x_b, y_b, z_b
	Axle boxes	x_{ab}, y_{ab}, z_{ab}
	Wheelsets	x_D, y_D, z_D
Longitudinal distance between:	Center of mass of the bogie frame and pivot	$x_{pi} = b_i$
	Pivot and wheelset	$x_{abij} = c$
	Pivot and body supports	$x_{spi} = f_1, f_2$
Vertical distance between:	Center of mass of the body, pivot and supports	$z_{spi} = h$
	Center of mass of the body and bogie frame	$z_{si} = h + h_1$
	Center of mass of the bogie frame, pivot and supports	$z_{sisp} = h_1$
	Center of mass of the bogie frame and wheelset	$z_{abij} = h_2$
Gaps	In the pivot assembly	Δ_p
	At the ends of the axle boxes	Δ_{ab}
	Between the wheel crest and the side face of the rail	Δ_c
Wheel radius	Medium	r_0
Transverse distance between:	Inner ends of wheels	$2S_c$
	Centers of axle boxes	$y_{abij} = 2d$
	Body supports	$y_{spi} = e$
	Center axes of rails	$2S$
Average radius of the curved section of the track		R
Raising the outer rail		ε
Angular velocity		Ω
Acceleration of gravity		g
Movement speed		V
Number of body supports on the bogie frame		n_o
Weights: body, bogie frame, wheelset		M, M_b, M_{ij}
Moments of inertia of masses relative to the corresponding axes		$I_x, I_z, I_{ix}, I_{iz}, I_{ijx}, I_{ijz}$
Stiffness coefficients and damping of the axle boxes with the bogie frame along the corresponding axes		$K_{ab\zeta}, K_{ab\eta}, K_{ab\zeta}, \beta_{ab\zeta}, \beta_{ab\eta}, \beta_{ab\zeta}$
Stiffness coefficients and damping coefficients of the body-bogie frame ligaments along and around the axes of their own coordinate systems		$K_{T\eta}, K_{T\zeta}, K_{T\varphi}, \beta_{T\eta}, \beta_{T\zeta}, \beta_{T\varphi}$
Taper profile of the wheel rim		λ
Friction force		T
Inner rail in a curved section of track		$k = 1$
Outer rail in a curved section of track		$k = 2$
Elastic squeezing of the rail: the difference in the moduli of the coordinate of the point of contact between the ridge and the rail in dynamics $ \eta_{Dijk} $, and the sum, consisting of the “arrow” of the arc of the curve, the gap $ \eta_{Nijk} $ in the track and unevenness of the rail in the plan		$\bar{y}_{ijk} = \eta_{Dijk} - \eta_{Nijk} $
Relative sliding speeds of wheels on rails in the directions of the corresponding coordinate axes		$\varepsilon_{\bar{\eta}}, \varepsilon_{\eta}$

Below, a modern-built undercarriage is considered, which has a two-stage body suspension and a frame suspension of traction electric motors (Fig. 1, 2). Electric and diesel trains EL2, DEL2, diesel locomotive TEP150, and other vehicles have similar undercarriage schemes.

In accordance with the Lagrange algorithm of the second kind (1), we determine the coordinates of the centers of mass and arbitrary points of the system components (Table 2).

The undercarriage, which is equipped with two-axle bogies, will have 17, and three-axle – 21 generalized coordinates.

Kinetic energy of the system is

$$T_K = \frac{1}{2} \times \left\{ M\dot{\eta}_0^2 + I_x\dot{\theta}^2 + I_z\dot{\phi}^2 + \sum_i \left\langle M_i \left(\dot{\eta}_o + \dot{y}_o + \dot{\phi} \cdot x_{oi} - \dot{\theta} \cdot z_{oi} \right)^2 + I_{ix} \left(\dot{\theta} + \dot{\theta}_i \right)^2 + I_{iz} \left(\dot{\phi} + \dot{\phi}_i \right)^2 \right\rangle + \sum_{ij} \left\langle M_{ij} \left[\dot{\eta}_o + \dot{y}_o + \dot{y}_{ij} + \dot{\phi} \cdot x_{oi} + x_{oij} - \dot{\theta} \cdot (z_{oi} + z_{oij}) + \dot{\phi}_i \cdot x_{oij} - \dot{\theta}_i \cdot z_{oij} \right]^2 + I_{ijx} \left(\dot{\theta} + \dot{\theta}_i \right)^2 + I_{ijz} \left(\dot{\phi} + \dot{\phi}_i + \dot{\phi}_{ij} \right)^2 \right\rangle \right\}. \quad (6)$$

Potential energy of the system

$$\Pi = \frac{1}{2} \left[K_{SP\eta} \cdot n_o \sum_i \eta_o^2 + K_{SP\eta} \cdot n_o \cdot x_i \sum_i \varphi^2 + K_{SP\zeta} \cdot n_o \sum_i (\theta \cdot e)^2 + K_{SP\eta} \cdot n_o \sum_i y_{oi}^2 + K_{SP\eta} \cdot n_o \cdot (f_1 + f_2) \sum_i \varphi_i^2 + K_{SP\zeta} \cdot n_o \sum_i (\theta_i \cdot y_{SPi})^2 + K_{ab} \sum_{ijk} (\theta_i d)^2 + K_{ab} \sum_{ijk} (\varphi_{ij} \cdot d)^2 + \left(\sum_i M_i y_{oi} + \sum_{ij} M_{ij} y_{oij} \right) \times (\varepsilon g - \Omega^2 R) + M(g \cdot \varepsilon - \Omega^2 R) z_{SPi} \right]. \quad (7)$$

System oscillation energy dissipation function

$$\Phi = \frac{1}{2} \left[\beta_{SP\eta} \cdot n_o \sum_i \dot{\eta}_o^2 + \beta_{SP\eta} \cdot n_o \cdot x_i \sum_i \dot{\varphi}^2 + \beta_{SP\zeta} \cdot n_o \sum_i (\dot{\theta} \cdot e)^2 + \beta_{SP\eta} \cdot n_o \sum_i \dot{y}_i^2 + \beta_{SP\eta} \cdot n_o \cdot (f_1 + f_2) \sum_i \dot{\varphi}_i^2 + \beta_{SP\zeta} \cdot n_o \sum_i (\dot{\theta}_i \cdot y_{SPi})^2 + \beta_{ab\zeta} \sum_{ijk} (\dot{\theta}_i d)^2 + \beta_{ab\zeta} \sum_{ijk} (\dot{\varphi}_{ij} \cdot d)^2 \right]. \quad (8)$$

According to the method of “virtual displacements” known from theoretical mechanics, the expressions of the generalized forces of the system acting in the directions of the corresponding coordinate axes are written. These include forces, the deformations of which have a nonlinear form, or contain gaps in the form of gaps, forces of preliminary tightening of elastic connections and friction between wheels and rails, disturbances from rail irregularities in the plane of the track [10]. In the mathematical model, these forces are highlighted in curly brackets.

Table 2

Coordinates of system components in the track coordinate system

Component	Centers of mass	Arbitrary points
Body	ξ	$\xi_k = \xi + x_o - \varphi y_o$
	η	$\eta_k = \eta + \varphi x_o + y_o - \theta z_o$
	ζ	$\zeta_k = \zeta + \theta y_o + z_o$
Bogie frame	$\xi_i = \xi + x_{oi}$	$\xi_{Ti} = \xi + x_{oi} + x_{Ti} - \varphi(y_{oi} + y_{Ti}) + \varphi y_{Ti}$
	$\eta_i = \eta + y_i + \varphi x_{oi} - \theta z_{oi}$	$\eta_{Ti} = \eta + y_i + \varphi(x_{oi} + x_{Ti}) - \theta(z_{oi} + z_{Ti}) - \theta_i z_{Ti}$
	$\zeta_i = \zeta + z_{oi}$	$\zeta_{Ti} = \zeta + z_{oi} + z_{Ti} + \theta(y_{oi} + y_{Ti}) + \theta_i y_i$
Wheelset	$\xi_{ij} = \xi + x_{oi} + x_{oij}$	$\xi_{Dij} = \xi + x_{oi} + x_{oij} + x_{Dij} - \varphi(y_{oi} + y_{oij} + y_{Dij}) - \varphi_i y_{Dij} + \varphi_{ij} y_{ij}$
	$\eta_{ij} = \eta + y_i + y_{ij} + \varphi(x_{oi} + x_{oij}) - \theta(z_{oi} + z_{oij}) + \varphi_i(x_{oij} + x_{Dij}) - \theta_i(z_{oi} + z_{oij}) - \theta_{ij} z_{Dij} + \varphi_{ij} x_{Dij}$	$\eta_{Dij} = \eta + y_i + y_{ij} + \varphi(x_{oi} + x_{oij} + x_{Dij}) - \theta(z_{oi} + z_{oij} + z_{Dij}) + \varphi_i(x_{oij} + x_{Dij}) - \theta_i(z_{oi} + z_{oij}) - \theta_{ij} z_{Dij} + \varphi_{ij} x_{Dij}$
	$\zeta_{ij} = \zeta + z_{oi} + z_{oij}$	$\zeta_{Dij} = \zeta + z_{oi} + z_{oij} + z_{Dij}$

The elastic push-out of the rail is calculated as the difference of the modules of the coordinate of the point of contact of the rim with rail in the dynamics $|\eta_{Dijk}|$, and the sum consisting of the “arrow” of the curve arc, gap $|\eta_{Nijk}|$ in the track, and the rail irregularities in the plan

$$\bar{y}_{ijk} = |\eta_{Dijk}| - |\eta_{Nijk}|. \quad (9)$$

For example, for the front (in the direction of travel) bogie, for its front wheelset, and the wheel rim running against the outer rail of a curved section of track, its deflection will be

$$\begin{aligned} \bar{y}_{112} &= |\eta_{D112}| - |\eta_{N112}| = \\ &= \left| \eta_o + y_{o1} + y_{o11} - S + \right. \\ &\quad \left. + \varphi(a_1 + c + a_{11}) + \theta(h + h_1 + h_2) + \right. \\ &\quad \left. + \varphi_1(b_1 + c + a_{11}) + \theta_1(h_2 + r_o) \right| - \\ &\quad \left| \frac{\varepsilon_{N112}^2}{2R} - A_{c2} \pm F_{112} - S \right|. \end{aligned} \quad (10)$$

After performing the operations, in accordance with (1), we obtain a system of differential equations, i.e., a mathematical model of vehicle dynamics (11):

$$\begin{aligned} 1. & \left(M + \sum_i M_i + \sum_{ij} M_{ij} \right) \ddot{\eta} + \\ & + \left[\sum_i M_i \cdot x_i + \sum_{ij} M_{ij} (x_i + x_{ij}) \right] \ddot{\varphi} - \\ & - \left[\sum_i M_i z_i + \sum_{ij} M_{ij} (z_i + z_{ij}) \right] \ddot{\theta} + \left(\sum_i M_i + \sum_{ij} M_{ij} \right) \ddot{y}_i + \\ & + \sum_{ij} M_{ij} x_{ij} \ddot{\varphi}_i - \sum_{ij} M_{ij} z_{ij} \ddot{\theta}_i + \sum_{ij} M_{ij} y_{ij} \ddot{\theta}_{ij} = n_o \beta_{SP\eta} \sum_i \dot{y}_i + \\ & + K_{SP\eta} n_o \sum_i y_i + M(g \cdot \varepsilon - \Omega^2 R) + F_A \varphi_A + \\ & + \left\{ \begin{aligned} & n_o K_{T\eta} y_i \delta_{1i} + P_{SP} \text{sign} y_i + P_p \text{sign} y_i \delta_{2i} + \\ & + \sum_i M_i \left[K_p \left(y_i + \varphi_i x_p - \theta_i z_{SPp} - l_{1i} \text{sign} y_i \right) \delta_{2i} + \right. \\ & \quad \left. + K_\infty \left(y_i + \varphi_i x_p - \theta_i z_p - l_{p2} \text{sign} y_i \right) \delta_{3i} \right] \end{aligned} \right\}, \end{aligned}$$

$$\begin{aligned}
 & 2. \left[I_z + \sum_i I_{iz} + \sum_{ij} I_{ijz} + \sum_i M_i \cdot x_i^2 + \sum_{ij} M_{ij} \cdot (x_i + x_{ij})^2 \right] \ddot{\varphi} + \\
 & + \left[\sum_i M_i \cdot x_i + \sum_{ij} M_{ij} \cdot (x_i + x_{ij}) \right] \ddot{y}_i + \\
 & + \sum_i \left[I_{iz} + \sum_{ij} I_{ijz} + \sum_{ij} M_{ij} \cdot x_{ij} (x_i + x_{ij}) \right] \ddot{\varphi}_i + \\
 & + M_{ij} \cdot z_{ij} \cdot (x_i + x_{ij}) \cdot \ddot{\theta}_i + M_{ij} \cdot (x_i + x_{ij}) \cdot \ddot{y}_{ij} + I_{ijz} \ddot{\varphi}_{ij} = \\
 & = \beta_{SP\eta} n_o \cdot x_i \sum_i \dot{\varphi}^2 + K_{SP\eta} n_o \cdot x_i \sum_i \varphi^2 + \\
 & + \left\{ \sum_i \left[\begin{aligned} & P_{SP} x_{SPi} \text{signy}_i + \\ & P_p \text{signy}_i \delta_{2i} + \\ & + K_p \left(y_i + \phi_i x_p - \theta_i z_p - l_{p1} \text{signy}_i \right) \delta_{2i} + \\ & + K_\infty \left(y_i + \phi_i x_p - \theta_i z_p - l_{p2} \text{signy}_i \right) \delta_{3i} \end{aligned} \right] x_{pi} + \right. \\
 & \left. + F_A l_A \varphi_A \right\},
 \end{aligned}$$

$$\begin{aligned}
 & 3. - \sum_i \left[M_i z_i + \sum_j M_{ij} \cdot (z_i + z_{ij}) \right] \ddot{\eta} + \\
 & + \left[I_x + \sum_i I_{ix} + \sum_{ij} I_{ijx} + \sum_i M_i \cdot z_i^2 + \sum_{ij} M_{ij} \cdot (z_i + z_{ij})^2 \right] \ddot{\theta} - \\
 & - \sum_i \left[M_i z_i + \sum_j M_{ij} \cdot (z_i + z_{ij}) \right] \ddot{y}_i - \\
 & - \left[\sum_{ij} M_{ij} \cdot (z_i + z_{ij}) x_{ij} \right] \ddot{\varphi}_i + \\
 & + \sum_i \left[I_{ix} + \sum_j M_{ij} \cdot (z_i + z_{ij}) \cdot z_i + \sum_j I_{ijx} \right] \ddot{\theta}_i - \\
 & - \sum_{ij} M_{ij} \cdot (z_i + z_{ij}) \ddot{y}_{ij} = \beta_{SP\zeta} n_o \sum_i y_{SPi}^2 \dot{\theta} + K_{SP\zeta} n_o \sum_i y_{SPi}^2 \theta - \\
 & - \left\{ \sum_i \left[\begin{aligned} & K_{SP\eta} n_o y_i \delta_{1i} + P_p \text{signy}_i \delta_{2i} + \\ & + K_p \left(y_i + \phi_i x_p - \theta_i z_p - l_{p1} \text{signy}_i \right) \delta_{2i} + \\ & + K_\infty \left(y_i + \phi_i x_p - \theta_i z_p - l_{p2} \text{signy}_i \right) \delta_{3i} \end{aligned} \right] \cdot z_{SPi} \right\},
 \end{aligned}$$

$$\begin{aligned}
 & 4; 7. \left(M_i + \sum_j M_{ij} \right) \ddot{\eta} - \left(M_i x_i + \sum_j M_{ij} x_{ij} \right) \ddot{\varphi} - \\
 & - \left[M_i z_i + \sum_j M_{ij} (z_i + z_{ij}) \right] \ddot{\theta} + \sum_j M_{ij} \ddot{y}_i + \\
 & + \left(\sum_j M_{ij} x_{ij} \right) \ddot{\varphi}_i - \sum_j M_{ij} z_{ij} \ddot{\theta}_i + \sum_j M_{ij} \ddot{y}_{ij} = \\
 & = \beta_{SP\eta} n_o \dot{y}_i + K_{SP\eta} n_o y_i + M_i (g \cdot \varepsilon - \Omega^2 R) + \\
 & + \sum_i P_{0p} \text{signy}_{pi} x_{SPi} + \\
 & + \left\{ \begin{aligned} & P_p \text{signy}_i \delta_{2i} + \\ & + K_p \left(y_i + \phi_i x_p - \theta_i z_p - l_{p1} \text{signy}_{pi} \right) \delta_{2i} + \\ & + K_\infty \left(y_i + \phi_i x_p - \theta_i z_p - l_{p2} \text{signy}_{pi} \right) \delta_{3i} \end{aligned} \right\} x_{pi} + \\
 & + \left\{ \begin{aligned} & P_{abij} \text{signy}_{ij} \delta_{ij1} + \\ & + K_{ab\eta} \left(y_{ij} - l_{ij1} \text{signy}_{pji} \right) \delta_{ij2} + \\ & + K_\infty \left(y_{ij} - l_{ij2} \text{signy}_{pji} \right) \delta_{ij3} \end{aligned} \right\} x_{abij}
 \end{aligned}$$

$$\begin{aligned}
 & 5; 8. \sum_j M_{ij} x_{ij} \ddot{\eta} + \left[I_{iz} + \sum_j I_{ijz} + \sum_j M_{ij} (x_i + x_{ij}) x_i \right] \ddot{\varphi} + \\
 & + \sum_j M_{ij} (z_i + z_{ij}) x_{ij} \ddot{\theta} + \sum_j M_{ij} (z_i + z_{ij}) x_{ij} \ddot{\theta}_i + \\
 & + \sum_j M_{ij} x_{ij} \ddot{y}_i + \left[I_{iz} + \sum_j (I_{ijz} + M_{ij} x_{ij}^2) \right] \ddot{\varphi}_i + \\
 & + \sum_j M_{ij} z_{ij} x_{ij} \ddot{\theta}_i + \sum_j M_{ij} x_{ij} \ddot{y}_{ij} + \sum_j I_{ijz} \ddot{\varphi}_{ij} = \\
 & = \beta_{SP\eta} n_o x_{SPi} \dot{\varphi}_i + K_{SP\eta} n_o x_{SPi} \varphi_i + \\
 & + \left\{ \begin{aligned} & P_p \text{signy}_i \delta_{2i} + \\ & + K_p \left(y_i + \phi_i x_p - \theta_i z_p - l_{p1} \text{signy}_i \right) \delta_{2i} + \\ & + K_\infty \left(y_i + \phi_i x_p - \theta_i z_p - l_{p2} \text{signy}_i \right) \delta_{3i} \end{aligned} \right\} + \\
 & + \left\{ \begin{aligned} & P_{abij} \text{signy}_{ij} \delta_{ij1} + K_{ab\eta} \left(y_{ij} - l_{ij1} \text{signy}_{ij} \right) \delta_{ij2} + \\ & + K_\infty \left(y_{ij} - l_{ij2} \text{signy}_{ij} \right) \delta_{ij3} \end{aligned} \right\} x_{abij}
 \end{aligned}$$

$$\begin{aligned}
 & 6; 9. - \sum_j M_{ij} z_{abij} \ddot{\eta} + \sum_j M_{ij} z_{abij} (x_i + x_{ij}) \ddot{\varphi} + \\
 & + \left\{ I_{ix} + \sum_j \left[I_{ijx} + M_{ij} z_{abij} (z_i + z_{abij}) \right] \right\} \ddot{\theta} - \\
 & - \sum_j M_{ij} z_{abij} \ddot{y}_i - \sum_j M_{ij} z_{abij} x_{ij} \ddot{\varphi}_i + \\
 & + \left[I_{ix} + \sum_j (I_{ijx} + M_{ij} z_{abij}^2) \right] \ddot{\theta}_i + \sum_j M_{ij} z_{abij} \ddot{y}_{ij} = \\
 & = \beta_{SP\zeta} n_o y_{SPi}^2 \dot{\theta}_i + \beta_{ab\zeta} y_{abij}^2 \dot{\theta}_i + K_{SP\zeta} n_o y_{SPi}^2 \theta_i + K_{ab\zeta} \sum_{jk} y_{abij}^2 \theta_i + \\
 & + \left\{ \begin{aligned} & P_p \text{signy}_i \delta_{2i} + \\ & P_{SP} \text{signy}_i z_{SISP} + \left[\begin{aligned} & + K_p \left(y_i + \phi_i x_p - \theta_i z_p - l_{p1} \text{signy}_i \right) \delta_{2i} + \\ & + K_\infty \left(y_i + \phi_i x_p - \theta_i z_p - l_{p2} \text{signy}_i \right) \delta_{3i} \end{aligned} \right] \times \\ & \times z_{Si} + \sum_{jk} \left[\begin{aligned} & P_{abij} \text{signy}_{ij} \delta_{ij1} + \\ & + K_{ab\eta} \left(y_{ij} - l_{ij1} \text{signy}_{ij} \right) \delta_{ij2} + \\ & + K_\infty \left(y_{ij} - l_{ij2} \text{signy}_{ij} \right) \delta_{ij3} \end{aligned} \right] z_{abij} \end{aligned} \right\},
 \end{aligned}$$

$$\begin{aligned}
 & 10; 11; 12; 13; 14; 15. M_{ij} \ddot{\eta} + M_{ij} \cdot (x_i + x_{ij}) \ddot{\varphi} - \\
 & - M_{ij} \cdot (z_i + z_{ij}) \ddot{\theta} + M_{ij} \ddot{y}_i + (M_{ij} x_{ij}) \ddot{\varphi}_i - M_{ij} z_{ij} \ddot{\theta}_i + M_{ij} \ddot{y}_{ij} = \\
 & = \left\{ \begin{aligned} & P_{abij} \text{signy}_{ij} \delta_{ij1} + \\ & \beta_p \cdot \ddot{y}_{ijk} (\delta_{ij1} + \delta_{ij2}) + \left[\begin{aligned} & + K_{ab\eta} \left(y_{ij} - l_{ij1} \text{signy}_{ij} \right) \delta_{ij2} + \\ & + K_\infty \left(y_{ij} - l_{ij2} \text{signy}_{ij} \right) \delta_{ij3} \end{aligned} \right] + \\ & + K_p \ddot{y}_{ijk} (\delta_{ij1} + \delta_{ij2}) + \sum_{ij} M_{ij} \cdot (g \cdot \varepsilon - \Omega^2 R) \end{aligned} \right\},
 \end{aligned}$$

$$\begin{aligned}
 & 16; 17; 18; 19; 20; 21. I_{ijz} \ddot{\varphi} + I_{ijz} \ddot{\varphi}_i + I_{ijz} \ddot{\varphi}_{ij} = \\
 & = -K_{ab\zeta} y_{abij}^2 \ddot{\varphi}_{ij} + T \left(\frac{\varepsilon_{\bar{\zeta}}}{\sqrt{\varepsilon_{\bar{\zeta}}^2 + \varepsilon_{\bar{\eta}}^2}} + \frac{\varepsilon_{\bar{\zeta}}}{\sqrt{\varepsilon_{\bar{\zeta}}^2 + \varepsilon_{\bar{\eta}}^2}} \right) + \\
 & + \sum_{jk} K_p \ddot{y}_{ijk} (\delta_{ij1} + \delta_{ij2}) f_c S_c. \quad (11)
 \end{aligned}$$

The mathematical model contains nonlinear differential equations with variable coefficients, the value of which is found at each integration step in accordance with the nonlinear characteristics of the connections. The model is compiled for a vehicle, the characteristics and geometry of which correspond to the drawing ones. The transition to a vehicle

with differences in design, characteristics, and geometry, which occurs during operation, is carried out by changing the coefficients.

Unlike previous versions [9, 10], this model has refined and more correctly compiled expressions for generalized forces and also takes into account the possibility of equipping the vehicle with a system for forced body tilt.

The verification (check of adequacy) of the mathematical model was carried out by comparing the dynamic indicators obtained in the process of mathematical modeling with the results of full-scale dynamic track tests of a diesel locomotive with a undercarriage similar to TEP150.

The elastic compressions of the outer rail when moving along curved sections of the track were compared; Fig. 4.

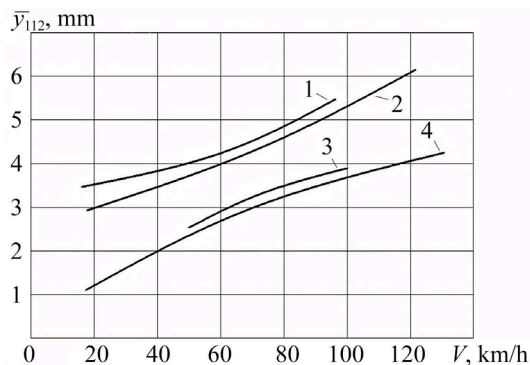


Fig. 4. Dependences of the external track rail deflections on the speed of movement in the curved section of the track of the first bogie of the first wheelset: 1, 2 – curve $R=350$ m; 3, 4 – curve $R=650$ m; rail elevation 0.15 m; 1, 3 – full-scale experiment; 2, 4 – calculation

Analysis of the dependences in Fig. 4 proves a sufficient coincidence of the calculated and experimental results, which indicates the adequacy of the mathematical model, which has improved somewhat compared to previous versions of the model. The experimental plots are located above the calculated ones: this is due to the fact that the vehicle moved along a real track, which has a wider range of excitations, which led to increased dynamic indicators.

5.2. Determining the dependence of wheel rim wear on speed

Ukrzaliznytsia has established speed limits on curved sections of the track, some of which reach almost 30%. Therefore, it is advisable to increase the speed on them in order to increase its average value. Let us examine the impact of increasing speed on some key indicators. The movement of a vehicle with a regular undercarriage and when equipped with one of the systems for radial installation of wheelsets (RIWS) when moving along a curved section of the track with a radius of 350 m, with an elevation of the outer rail of 0.15 m, is considered. Here, the speed is limited to 70 km/h, provided that the safety of movement is ensured by the creeping of the rim onto the rail.

Fig. 5 shows the dependence of the relative wear of wheel rim of the first bogie of the first wheelset, which runs into the outer rail of the curved section of the track, on the speed of movement. The relative wear is taken as the ratio of the calculated thickness of the rim to its average statistical value, which for traction rolling stock is estimated at approximately 1 mm/10 thousand km of mileage. The following are indicat-

ed: plot 1 is a standard vehicle; plot 2 is a vehicle equipped with a system of radial self-installation of wheelsets; plot 3 is a vehicle equipped with a forced radial installation system of wheelsets; 4, 5 – speed limits for traffic safety; 6 – limits for permissible wear of wheel rims.

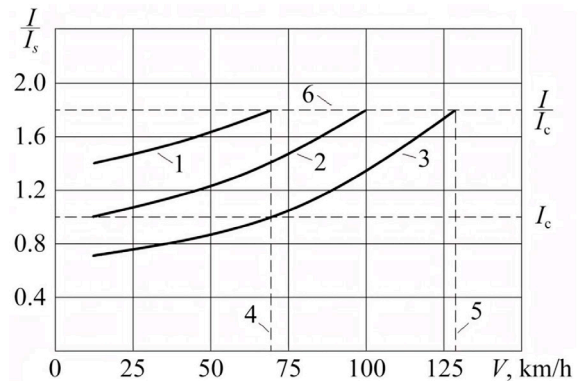


Fig. 5. Dependences of the relative wear of a wheel rim of the first bogie of the first wheelset running onto the outer rail of a curved section of the track on the speed of movement

As can be seen from plots 1–3, Fig. 5, the radial self-adjustment system of wheelsets (RSASW) provides a reduction in the relative wear of rims at all speeds up to 24%, and the forced adjustment system (SFIWS) – up to 50%.

The dependence of the undamped acceleration in the vehicle body on the speed of movement along a curved section of the track with a radius of 350 m, and with an increase in the outer rail of 0.15 m, is shown in Fig. 6.

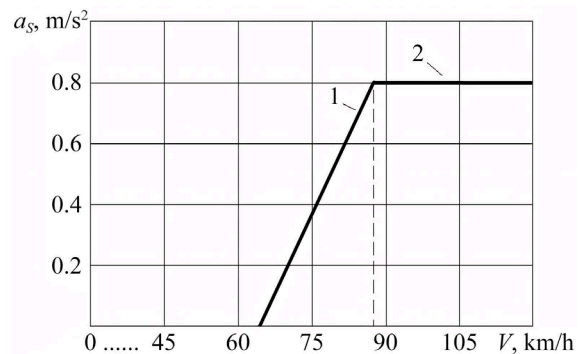


Fig. 6. Dependence of the magnitude of undamped acceleration in the vehicle body on the speed of movement along the curve of the track section: 1 – standard; 2 – equipped with a forced body tilt system

As can be seen from the plots in Fig. 6, the speed limit occurs at 88 km/h. To maintain the undamped acceleration at this level, it is necessary to install a system on the vehicle for lateral tilting of the vehicle body to a certain angle – in addition to its tilting due to the increase in the outer rail in the curve of the track section

$$a_s = \frac{V^2}{R} - g \left(\frac{\varepsilon + \varepsilon_{II} \cdot \delta_{II}}{2S} \right) \leq 0.8, \quad (12)$$

where ε_{II} – increase in the height of body supports from the side of the outer rail; δ_{II} – control function that determines the beginning and end of the action of the device for forced body tilt:

$$a_s < 0.8 \text{ m/s}^2; \text{ then } \delta_{II} = 0, \quad (13)$$

$$a_s \geq 0.8 \text{ m/s}^2; \text{ then } \delta_{II} = 1.$$

When implementing the body tilt, taking into account the conditions of fitting into the dimensions, the angle of its rotation around the longitudinal axis, which passes through the supports on the side of the inner rail of the curved section of the track, is

$$\theta_{II} = \frac{\varepsilon_{II}}{2S} \delta_{II} < 7^\circ. \quad (14)$$

The angle θ_{II} should not exceed 7 degrees, so the speed is limited to 120 km/h (Fig. 6).

Table 3 gives a comparison of the characteristics of the movement of a modern high-speed train with similar but equipped with forced systems for radial installation of wheelsets and body tilt. Movement on a track section 500 km long is considered, of which 10% are curved sections with a radius close to 350 m, and an increase in the outer rail of 0.15 m. Time spent at stops, changes in speed during acceleration and braking were neglected.

As can be seen from Table 3, we have significant increases in average train speed and reduction in travel time if the proportion of curved sections on the section is greater than 30%.

A second task is to ensure passenger comfort, which is assessed in particular by the magnitude of the component of undamped acceleration transverse to the track. It is known that this task can be solved by forcing the lateral inclination of the vehicle body to a certain angle – in addition to its inclination by raising the outer rail in the curved section of the track.

The dependence of undamped acceleration on the speed of movement along the curved section of the track in the body of a standard vehicle (1) is practically linear (Fig. 6). In a curve with a radius of 350 m with an increase in the outer rail of 0.15 m, the component of undamped acceleration transverse to the track reaches the permissible value (0.8 m/s²) already at a speed of movement $V = 88 \text{ km/h}$.

Equipping the vehicle with a system of forced lateral tilt of the vehicle body makes it possible to stabilize the undamped acceleration at an acceptable level (0.8 m/s²), i.e., comfortable conditions for passengers are provided: (line 2).

Therefore, the simultaneous use of forced systems of RIWS and body tilt on curved sections of the track with a radius close to 350 m and an increase in the outer rail of 0.15 m makes it possible to significantly (by 25 min, i.e., by 8.3%) reduce the total train travel time.

Our research results have certain advantages in comparison with known ones.

Table 3

Comparison of train movement characteristics

Train	Length of straights/average speed of movement/time of movement	Curve length/Average travel speed/Travel time	Average speed, km/h	Total time of movement, hours (hours, minutes)
Modern high-speed train	450 km	50 km	100.0	5.0 h
	104.9 km/h	70 km/h		
	4.29 h	0.71 h		
Train with forced systems for radial installation of wheelsets in curves and body tilt; Curve length 10%	450 km	50 km	106.0	4.71 h (4 h 43 min)
	104.9 km/h	120 km/h		
	4.29 h	0.42 h		
Curve length 30%	350 km	150 km	109.0	4.59 h (4 h 35 min)
	104.9 km/h	120 km/h		
	3.34 h	1.25 h		

Unlike the results reported in [1–3], issues related to the problems of operation of rolling stock have been highlighted.

Unlike the findings from [4, 5], issues related to the problems of vehicle movement on curved sections of the track have been highlighted.

Unlike the results in [6], we have designed the system of forced body tilt for moving on curves that is simpler in terms of structure and operation; a patent application was filed.

Unlike the findings of [7], overcoming obstacles in the implementation of high-speed movement on UZ is proposed by using domestic developments of RIWS systems and forced body tilt.

Unlike the results from [6], modeling was carried out under the action of excitation from rails on the vehicle.

Unlike the findings reported in [8–10], sufficient attention has been paid to checking the adequacy of mathematical modeling of vehicle movement, taking into account train movement modes, as well as the prospect of increasing vehicle movement speeds.

Almost 50 years of experience in using RIWS and body tilt systems on curved sections of the track in Switzerland, Norway, etc. proves their high efficiency in solving the problems of rim wear and passenger comfort.

The effectiveness of the application of our results is limited by the condition that the track and high-speed vehicles operating on it are maintained in excellent condition.

The disadvantages of this study are the lack of checks of the stability margin and robustness (roughness) of the synthesized mathematical model.

6. Discussion of results related to vehicle motion modeling

The experimental plots (Fig. 4) are located higher than the calculated ones. This is due to the fact that during dynamic track tests, the vehicle moved along a real track, which caused higher values of dynamic indicators.

Fig. 5 shows plots that demonstrate the increase in the relative wear of the vehicle wheel rims with increasing speed. When equipping the vehicle with RIWS systems, relative wear decreases at all speeds. This allows one to increase the vehicle speed from 70 km/h (plot 1) to 100 km/h (plot 2) when using RSASW.

A much greater effect can be achieved if one equips the vehicle with an SFIWS system, which allows one to increase the speed to 136 km/h (plot 3, Fig. 5). Line 6, Fig. 5 – speed limit for relative wear of the rims.

Therefore, RIWS systems provide the opportunity to significantly increase the average speed of vehicles – without exceeding the average amount of tread wear.

Our work in the future involves refining the calculated parameters of the research object and the disturbances coming from the track during the movement of high-speed vehicles.

7. Conclusions

1. A calculation scheme of the vehicle undercarriage containing linear and nonlinear relationships between its masses has been drawn up; the working hypotheses and assumptions were defined. The track was represented in the form of two elastic beams with irregularities located on a transversely elastic-viscous base. The elastic rail push-off was calculated as the difference between the modules of the coordinate of the contact point of the rim with the rail in dynamics and the sum consisting of the “arrow” of the curve arc, the gap in the track and the rail roughness in the plan. The forces at the wheel-rail contacts were calculated according to the creep theory and the dry friction hypothesis. The reaction from the cars applied to the vehicle’s automatic coupling was taken into account. A mathematical model of the dynamics of the high-speed vehicle was synthesized, which consists of nonlinear differential equations with variable coefficients; the damping coefficients were considered constant. Equations of the connections take into account possible deviations in their geometry and characteristics from the drawing ones in operation. Testing has proven a sufficient coincidence of the calculated and experimental dynamics indicators, which indicates the adequacy of this version of the mathematical model, which has improved somewhat compared to the previous ones.

2. Equipping a vehicle with a system for radial self-alignment of wheelsets makes it possible, on a curve with a radius of 350 m and an increase in the outer rail of 0.15 m, to increase the speed from 70 to 100 km/h. When equipped with a system for forced radial alignment of wheelsets, under these conditions, the speed can be increased from 70 to 136 km/h. The relative wear of wheel rims on this curved section of the track remains at the level of 1.8 mm/10 thousand km of run. Equipping a vehicle with a system for forced body tilt makes it possible, on a curve with a radius of 350 m and an increase in the

outer rail of 0.15 m, to increase the speed from 88 to 120 km/h. Therefore, it is advisable to simultaneously equip vehicles with systems for forced radial installation of wheelsets and body tilt on a route that contains 30% of curves with a radius of approximately 350 m. This will reduce train travel time by 8.3%. The percentage will increase proportionally – in accordance with the increase in the length of curved sections of the track along the route.

Conflicts of interest

The authors declare that they have no conflicts of interest in relation to the current study, including financial, personal, authorship, or any other, that could affect the study, as well as the results reported in this paper.

Funding

The study was conducted without financial support.

Data availability

All data are available, either in numerical or graphical form, in the main text of the manuscript.

Use of artificial intelligence

The authors confirm that they did not use artificial intelligence technologies when creating the current work.

Acknowledgments

The authors are sincerely grateful to Professor Viktor Vanin for his useful suggestions on determining the coefficients for the differential equations of the mathematical model.

References

1. Lawrence, M., Bullock, R., Liu, Z. (2019). China’s High-Speed Rail Development. Washington, DC: World Bank. <https://doi.org/10.1596/978-1-4648-1425-9>
2. Huang, Y., Zong, H. (2020). The spatial distribution and determinants of China’s high-speed train services. *Transportation Research Part A: Policy and Practice*, 142, 56–70. <https://doi.org/10.1016/j.tra.2020.10.009>
3. Tkachenko, V., Sapronova, S., Braikovska, N., Tverdomed, V. (2021). Dynamic interaction of rolling stock and track on lines of speed motion combined with freight. Vinnytsia: NGO “European Scientific Platform”. <https://doi.org/10.36074/dvrsklshrsrv-monograph.2021>
4. Hubar, O., Markul, R., Tiutkin, O., Andrieiev, V., Arbuzov, M., Kovalchuk, O. (2020). Study of the interaction of the railway track and the rolling stock under conditions of accelerated movement. *IOP Conference Series: Materials Science and Engineering*, 985 (1), 012007. <https://doi.org/10.1088/1757-899x/985/1/012007>
5. Matej, J. L., Orliński, P. (2023). Reducing wheel wear of a motorised metro car on a curved track with a small curve radius. *Rail Vehicles/Pojazdy Szynowe*, 3-4, 25–32. <https://doi.org/10.53502/rail-175921>
6. Yeritsyan, B., Liubarskyi, B., Iakunin, D. (2016). Simulation of combined body tilt system of high-speed railway rolling stock. *Eastern-European Journal of Enterprise Technologies*, 2 (9 (80)), 4–17. <https://doi.org/10.15587/1729-4061.2016.66782>
7. Lin, Y., Qin, Y., Xie, Z. (2021). Does foreign technology transfer spur domestic innovation? Evidence from the high-speed rail sector in China. *Journal of Comparative Economics*, 49 (1), 212–229. <https://doi.org/10.1016/j.jce.2020.08.004>
8. Gerlici, J., Lovska, A., Pavliuchenkov, M. (2024). Study of the Dynamics and Strength of the Detachable Module for Long Cargoes under Asymmetric Loading Diagrams. *Applied Sciences*, 14 (8), 3211. <https://doi.org/10.3390/app14083211>
9. Masliev, V. G., Kalinina, S. A., Yakunin, D. I. (2000). Bazovaya matematicheskaya model’ gorizonta’l’noy dinamiki lokomotiva. *Visnyk Kharkivskoho politekhnichnoho universytetu*, 118, 17–20.
10. Masliev, V. G. (2008). *Dinamika teplovozov s ustroystvami, umen’shayuschimi iznos bandazhey koles*. Kharkiv: NTU «KhPI», 288.